



Synthesis, structure, molecular docking, and structure–activity relationship analysis of enamines: 3-Aryl-4-alkylaminofuran-2(5H)-ones as potential antibacterials

Zhu-Ping Xiao^{a,b,*}, Xing-Bing He^c, Zhi-Yun Peng^a, Tao-Ju Xiong^d, Juan Peng^d, Li-Hua Chen^a, Hai-Liang Zhu^{a,b,*}

^a College of Chemistry and Chemical Engineering, and Key Laboratory of Hunan Forest Products and Chemical Industry Engineering, Jishou University, Jishou 416000, PR China

^b State Key Laboratory of Pharmaceutical Biotechnology, Nanjing University, Nanjing 210093, PR China

^c College of Biology and Environmental Sciences, Jishou University, Jishou 416000, PR China

^d Xiangxi Autonomous Prefecture People's Hospital, Jishou 416000, PR China

ARTICLE INFO

Article history:

Received 2 December 2010

Revised 24 January 2011

Accepted 25 January 2011

Available online 1 February 2011

Keywords:

3-Aryl-4-alkylaminofuran-2(5H)-one

Antibacterial

Molecular docking

Tyrosyl-tRNA synthetase

Structure–activity relationship

ABSTRACT

Thirty-one 3-aryl-4-alkylaminofuran-2(5H)-ones were designed, prepared and tested for their antibacterial activity. Some of them showed significant antibacterial activity against Gram-positive organisms, especially against *Staphylococcus aureus* ATCC 25923, but all were inactive against Gram-negative organisms. Out of these compounds, 3-(4-bromophenyl)-4-(2-(4-nitrophenyl)hydrazinyl)furan-2(5H)-one (**4a11**) showed the most potent antibacterial activity against *S. aureus* ATCC 25923 with MIC₅₀ of 0.42 µg/mL. The enzyme assay revealed that the possible antibacterial mechanism of the synthetic compounds might be due to their inhibitory activity against tyrosyl-tRNA synthetase. Molecular dockings of **4a11** into *S. aureus* tyrosyl-tRNA synthetase active site were also performed. This inhibitor snugly fitting the active site might well explain its excellent inhibitory activity. Meanwhile, this modeling disclosed that a more suitable optimization strategy might be to modify the benzene ring at 3-position of furanone with hydrophilic groups.

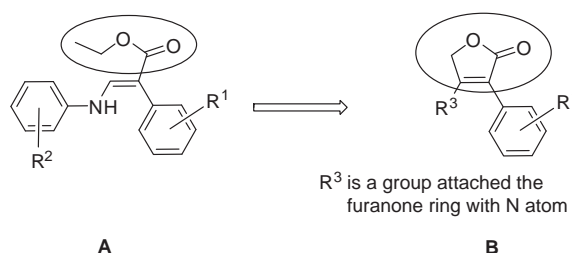
© 2011 Elsevier Ltd. All rights reserved.

1. Introduction

Bacterial resistance to the available drugs provides physicians with a real challenge to the effective treatment of infectious diseases and poses a serious threat to human health. Although a more appropriate use of current antibacterial agents will result in a reduction of the resistance phenomenon, the development of new antibacterial agents appears to be the most attractive challenge to fight against the emergence of resistance.¹ Modification of known antibacterial scaffolds is becoming increasingly difficult to deliver new leads. The focus of much antibacterial research has, therefore, moved to the identification and development of new structural classes of antibacterial agents.²

We recently found that 2-aryl-3-arylaminoacrylates have potent antibacterial activity against *Staphylococcus aureus* with *E*-configuration exhibiting much higher antibacterial activity than the corresponding *Z*-isomer.^{3,4} Furthermore, *E*-isomers have a risk of isomerization to *Z*-isomers at low pH. Therefore, we shifted our focus to design and synthesis of an enamine with *E*-configuration

being the only possible isomer as a means of enhancing efficacy. The strategy employed is to form a ring between the ester moiety of (*E*)-ethyl 2-aryl-3-arylaminoacrylate (**A**) and the double bond, resulting in compound **B** with a furan-2(5H)-one core (Scheme 1). Furan-2(5H)-ones showed many biological activities, such as being inhibitors of HIV-1 integrase⁵ as well as antibacterial,⁶ antioxidant,^{7,8} anti-pyretic,⁹ anti-osteoporosis,¹⁰ and anti-inflammatory agents.^{7,8} Herein, we reported furan-2(5H)-ones (**B**) with an aliphatic amino group as antibacterials and the compounds with an aryl amino group will be reported elsewhere. The possible mechanism of their antibacterial action was also discussed.



Scheme 1.

* Corresponding authors. Tel./fax: +86 743 8563911 (Z.-P.X.); tel.: +86 25 8359 2572; fax: +86 25 8359 2672 (H.-L.Z.).

E-mail addresses: xiaozhuping2005@163.com (Z.-P. Xiao), zhuhl@nju.edu.cn (H.-L. Zhu).

2. Results and discussion

2.1. Chemistry

Thirty-one 3-aryl-4-alkylaminofuran-2(5*H*)-ones were designed and synthesized by the routes outlined in Scheme 2. Synthesis of the 3-aryl-4-alkylaminofuran-2(5*H*)-ones (**4a1–4a11**, **4b1**, **4c1**, **4d1–4d9**, **4e1–4e8**) required first the synthesis of chlorohydrocarbon **3** which was obtained by chloration of **2** with PCl_3 in the presence of *N,N*-dimethylformamide (DMF) in Et_2O . Chlorohydrocarbon **3** was then aminated in dry THF with an appropriated amine to give the desired product **4** (Scheme 2). The intermediates **2** were synthesized according to the previously reported method with some modifications.⁷ In brief, base-catalyzed esterification of an appropriately substituted phenylacetic acid with ethyl bromoacetate yielded ester **1** using sodium ethoxide in ethanol. Furanone **2** was then obtained by the Dieckmann ester condensation of **1** at the presence of sodium hydride in dry THF. All 3-aryl-4-alkylaminofuran-2(5*H*)-ones were first reported and were fully characterized by spectroscopic methods and elemental analysis together with a crystal structure (**4a9**).

2.2. Description of the crystal structure

Compound **4a9** was determined by X-ray diffraction analysis. The crystal data are presented in Table 1 and some important bond lengths are given in Table 2. As shown in Fig. 1, **4a9** crystallized with two chemically equivalent but crystallographically distinct molecules per asymmetric unit. To simplify the description, we represent them as units A (containing Br1) and B (containing Br2), respectively. Within the A and B units, both bond lengths and angles are almost identical, but the molecules run along different directions which make an angle of $50.0(2)^\circ$. The bond C7–C10 ($1.375(4)\text{Å}$) was assigned as a double bond,^{11,12} and compound **4a9** was therefore identified as a furan-2(5*H*)-one not a furan-2(3*H*)-one. ^1H NMR spectrum of **4a9** provides another evidence for this assignment. For the lactone moiety, the ^1H NMR spectrum displayed the two proton signals as singlet at about δ_{H} 5.06. Comparing ^1H NMR spectra of **4a9** with those of other compounds, all synthetic compounds were determined as 3-aryl-4-alkylaminofuran-2(5*H*)-ones. C10–N1 ($1.333(3)\text{Å}$) bond has a shorter bond distance than the standard C–N single bond (1.46Å),¹³ but longer than C–N double bond (1.27Å).¹⁴ This strongly indicates that the

Table 1

Crystal structure data for **4a9**

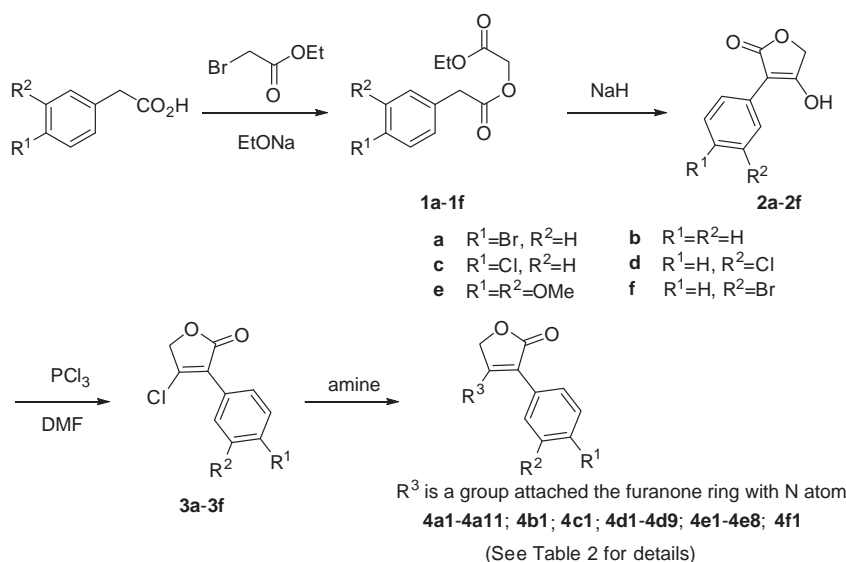
Compounds	4a9
Formula	$\text{C}_{12}\text{H}_{12}\text{BrNO}_2$
Mr	282.14
Crystal size (mm^3)	$0.20 \times 0.20 \times 0.10$
Crystal system	Monoclinic
Space group	$P2_1/n$
<i>a</i> (Å)	16.0128(9)
<i>b</i> (Å)	8.8528(5)
<i>c</i> (Å)	17.6007(10)
<i>V</i> (Å ³)	2353.6(2)
<i>Z</i>	8
<i>D_c</i> (g/cm^{-3})	1.592
μ (mm^{-1})	3.477
<i>F</i> (0 0 0)	1136
Max. and min. trans.	0.7224 and 0.5431
θ range ($^\circ$)	2.10/28.26
Index range (<i>h, k, l</i>)	–21/21, –11/11, –23/23
Reflections collected/unique	28164/5830
Data/restraints/parameters	5830/0/293
<i>R_{int}</i>	0.0368
Goodness-of-fit on <i>F</i> ²	1.052
<i>R</i> ₁ , <i>wR</i> ₂ [<i>I</i> > 2σ(<i>I</i>)]	0.0481/0.1175
<i>R</i> ₁ , <i>wR</i> ₂	0.0700/0.1307
Extinction coefficient	–
(Δρ) _{max} , (Δρ) _{min} . ($\text{e}/\text{Å}^3$)	0.429/–1.207

Table 2

Important bond lengths (Å) of compound **4a9**

Bond	Bond length
C1–C7	1.472(4)
C7–C8	1.437(4)
C7–C10	1.375(4)
C9–C10	1.502(4)
C10–N1	1.333(3)
C11–N1	1.456(4)

p orbital of N1 seems to be conjugated with the π molecular orbital of C7–C10 double bond, which is supported by the torsion angle of C8–C7–C10–N1 ($-172.8(3)^\circ$) being small deviation from 180° . The C–C double bond attached by a nitrogen atom clearly indicates that compound **4a9** is an enamine.



Scheme 2.

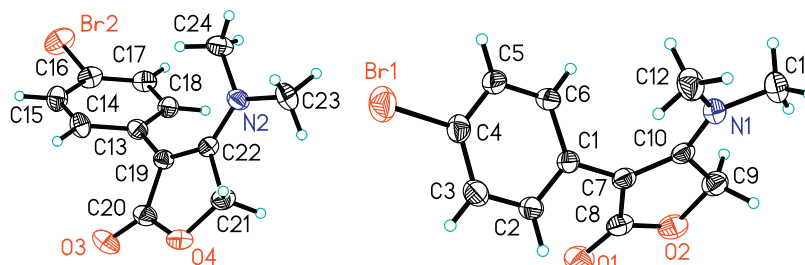


Figure 1. Molecular structure of compound **4a9** which crystallizes with two molecules per asymmetric unit, showing the atom-numbering scheme. Displacement ellipsoids are drawn at the 30% probability level.

The stereochemistry of the double bond in furanone ring was assigned as *E*-configuration based on X-ray crystallography of product **4a9** (Fig. 1). This provides a basis for assigning the *E*-configuration to all newly synthetic 3-aryl-4-alkylaminofuran-2(5*H*)-ones.

2.3. Antibacterial activity

All synthetic compounds were evaluated for their antimicrobial activities against three Gram-positive organisms (*Bacillus subtilis* ATCC 6633, *S. aureus* ATCC 25923, *Candida albicans* ATCC 10231) and a Gram-negative organism (*Escherichia coli* ATCC 35218), and the results are presented in Table 3. The first information obtained in this study is that some of the tested compounds showed good activities against Gram-positive organisms, and all of them were inactive against Gram-negative organism (*E. coli* ATCC 35218). The second is that, of the three Gram-positive strains, *S. aureus* ATCC 25923 was the most sensitive to these compounds. The structure–activity relationships were therefore established from the antibacterial data against *S. aureus* ATCC 25923.

The first set of analogues that were prepared are 4-bromophenyl derivatives (**4a1–4a11**), the aim which was to explore the role of R^3 (Scheme 2) on the antibacterial activity. Compound containing a 1-pyrrolidinyl (**4a1**), 4-morpholinyl (**4a3**), 1-piperazinyl (**4a4**), cyclohexylamino (**4a6**) or benzylamino (**4a10**) group was slightly less active than compound **4a2**, while the propylamino (**4a7**), butylamino (**4a8**) and *N,N*-dimethylamino (**4a9**) analogues showed significant decreases in activity. This indicates that R^3 bearing a ring is favorable for antibacterial activity against *S. aureus*. On the contrary, substitution at R^3 position with a morpholinylethylamino (**4a5**) or a *p*-nitrophenylhydrazino (**4a11**) group led to an over 2- or 50-fold increase in activities by comparison with **4a2**. Out of the compounds tested, **4a11** was the most active with MIC₅₀ of 0.42 µg/mL, displaying higher level of antibacterial activity than that of the commercial antibiotic, kanamycin (MIC₅₀ = 1.0 µg/mL). Variation of R^3 led to compounds (**4a1–4a11**) with MIC₅₀ values differed greatly, ranging from 0.42 to >100 µg/mL. This indicates that R^3 seems to be more suitable for further modification.

We next prepared several sets of analogues (Table 3) by modification of the benzene ring at C3 in furanone moiety. Both removal and replacement of the 4-bromo group led to compounds with reduced activity (**4a11** vs **4b1**, **4a1** vs **4c1**). However, shifting substituent atom from 4-position (**4a9** or **4c1**) to 3-position (**4f1** or **4d1**) resulted in a significant increase in antibacterial activity, indicating that the modification in position 3 would result in compounds with improved activity. Compounds (**4e1–4e8**), which introduced methoxy groups at 3,4-positions in benzene ring, showed a dramatic loss in activity compared to the analogues bearing only one substituent (**4a1–4a11**, **4d1–4d9**). Based on these results, further modification at position 3 in benzene fragment and at R^3 position (Scheme 2) is undergoing.

2.4. Inhibitory activities of 3-aryl-4-aminofuran-2(5*H*)-ones against tyrosyl-tRNA synthetase from *S. aureus*

To explore the possible antibacterial mechanism of the synthetic compounds, many antibacterial agents with clear mechanism were used to overlap with the most potent compound (**4a11**) based on the energy-minimized conformation. It turns out that conformation of **4a11** is very similar to SB-239629 (Scheme 3, Fig. 2), which leads to a conception that 3-aryl-4-aminofuran-2(5*H*)-one would be a novel tyrosyl-tRNA synthetase inhibitor. Compound SB-239629,¹⁵ a semi-synthetic derivative¹⁶ of SB-219383 which is a naturally occurring antibiotic,¹⁷ shows significant inhibitory activity against tyrosyl-tRNA synthetase (IC₅₀ = 3 nM).^{15,16} Unfortunately, SB-239629 exhibited only weak antibacterial activity (MIC over 64 µg/mL against *Streptococcus pneumoniae* R6¹⁶) due to its highly polar nature, which leads to a poor penetration of bacterial cells.¹⁷ It is well known that tyrosyl-tRNA synthetase is one of the aminoacyl-tRNA synthetases which are responsible for maintaining the fidelity of transfer of genetic information from DNA into protein by producing charged tRNAs.^{18–20} These enzymes are essential for cell viability, and they are potential targets for antibacterial agents. This concept is proven by the success of the broad-spectrum antibacterial drug mupirocin, which targets bacterial isoleucyl-tRNA synthetases.²¹

Based on the above mentioned, compounds with MIC₅₀ <30 µg/mL were therefore evaluated for inhibitory activity against tyrosyl-tRNA synthetase from *S. aureus* and the results are presented in Table 4. The results revealed that the potent antibacterial agents (**4a11**, **4b1**, and **4d6**) also exhibited strong inhibition against this enzyme, with **4a11** being the most active and achieving IC₅₀ as low as 0.12 ± 0.04 µM. An obvious correlation was found between the IC₅₀ values in the enzyme assay and the MIC₅₀ values against whole cell.

2.5. Molecular docking

With in vitro activity against tyrosyl-tRNA synthetase from *S. aureus* in hand, it is thought worth-while to do molecular docking studies to support the potency of inhibition. To this end, molecular docking of the most potent inhibitor **4a11** into SB-239629 binding site of tyrosyl-tRNA synthetase was performed on the binding model based on the tyrosyl-tRNA synthetase complex structure (1jjj.pdb).¹⁵ The interactions between compound **4a11** and the active site residues of tyrosyl-tRNA synthetase are shown in Fig. 3.

In the binding model, **4a11** locates in the substrate binding site of tyrosyl-tRNA synthetase, with its O atom in furanone ring forming hydrogen-bonding interactions with the backbone amino groups of Gly193 (1.939 Å), while the NH group attached to furanone ring forms another hydrogen-bond with the carbonyl group of Gly38, having the H···O bond length of 2.062 Å. Compound **4a11** interacts with the side chain of Thr75 via two O–H···O

Table 3
Inhibitory activity (IC₅₀) of the synthetic compounds against microbes

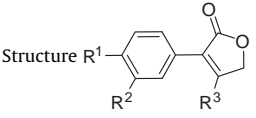
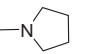
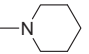
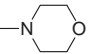
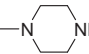
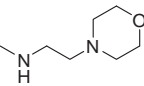
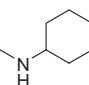
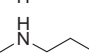
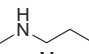
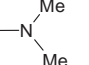
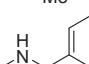
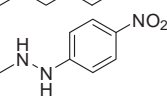
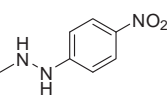
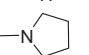
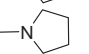
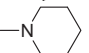
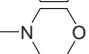
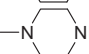
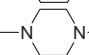
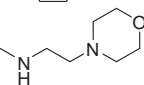
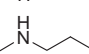
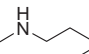
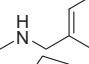
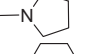
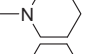
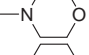
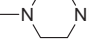
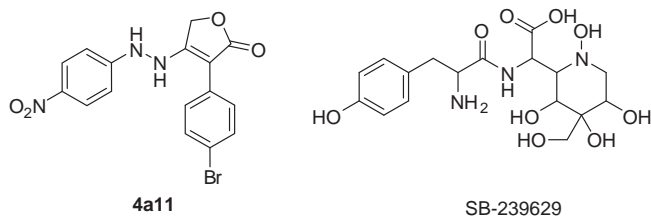
Compounds	Structure 			MIC ₅₀ (μg/mL)			
	R ¹	R ²	R ³	A	B	C	D
4a1	Br	H		50	37.1	49.8	>100
4a2	Br	H		>100	21.8	74.4	>100
4a3	Br	H		91.8	42.6	89.7	>100
4a4	Br	H		78.5	54.7	77.4	>100
4a5	Br	H		24.7	9.7	3.5	>100
4a6	Br	H		86.7	27.8	62.8	>100
4a7	Br	H		>100	87.2	>100	>100
4a8	Br	H		>100	>100	>100	>100
4a9	Br	H		>100	>100	>100	>100
4a10	Br	H		>100	57.6	>100	>100
4a11	Br	H		9.5	0.42	5.2	79.4
4b1	H	H		15.6	0.85	13.1	>100
4c1	Cl	H		>100	88.4	>100	>100
4d1	H	Cl		87.4	12.6	71.2	>100
4d2	H	Cl		41.6	7.5	33.1	>100
4d3	H	Cl		93.1	25.7	74.6	>100
4d4	H	Cl		>100	37.4	>100	>100
4d5	H	Cl		>100	65.2	>100	>100
4d6	H	Cl		27.9	3.2	21.3	>100
4d7	H	Cl		>100	52.4	>100	>100
4d8	H	Cl		>100	>100	9.08	>100
4d9	H	Cl		>100	25.3	83.9	>100
4e1	MeO	MeO		>100	>100	>100	>100
4e2	MeO	MeO		>100	>100	>100	>100
4e3	MeO	MeO		>100	>100	>100	>100
4e4	MeO	MeO		>100	>100	>100	>100

Table 3 (continued)

Compounds	Structure			MIC ₅₀ (μg/mL)			
	R ¹	R ²	R ³	A	B	C	D
4e5	MeO	MeO		>100	>100	>100	>100
4e6	MeO	MeO		>100	68.3	>100	>100
4e7	MeO	MeO		>100	>100	>100	>100
4e8	MeO	MeO		>100	>100	>100	>100
4f1	H	Br		>100	61.4	>100	>100
Kanamycin				0.43	1.0	—	—
Penicillin				—	—	—	2.5
Ketoconazole				—	—	4.4	—

Note: (A) *B. subtilis* ATCC 6633; (B) *S. aureus* ATCC 25923; (C) *C. albicans* ATCC 10231; (D) *E. coli* ATCC 35218.



Scheme 3.

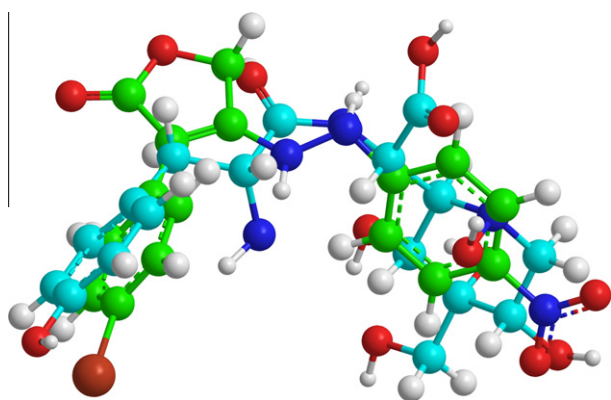


Figure 2. Conformation overlap between SB-239629 (cyan) and a 3-aryl-4-arylamino-2(5H)-furanone (**4a11**, green).

hydrogen bonds with H···acceptor distances of 2.188 and 1.830 Å, respectively. The modeling also suggested that there was a H–π interaction (3.422 Å) between the benzene ring of *p*-nitrophenylhydrazino moiety of **4a11** and amino group of Gln174. In addition to the strong stabilizing H-bond interactions, the higher affinity of **4a11** might also be accounted for by some hydrophobic interactions. As an example, the spatially close residue Thr42 forms a hydrophobic interaction with the bromine atom of **4a11**. The above mentioned interactions tightly anchoring **4a11** to the active

Table 4

In vitro inhibitory activity data of the synthesized compounds against *S. aureus* methionyl-tRNA synthetase

Compound	IC ₅₀ (μM)
4a2	7.7 ± 1.3
4a5	3.3 ± 0.6
4a6	14.5 ± 3.7
4a11	0.12 ± 0.04
4b1	0.24 ± 0.06
4d1	5.6 ± 1.1
4d2	2.8 ± 0.7
4d3	10.8 ± 1.8
4d6	0.86 ± 0.09
4d9	8.9 ± 1.4

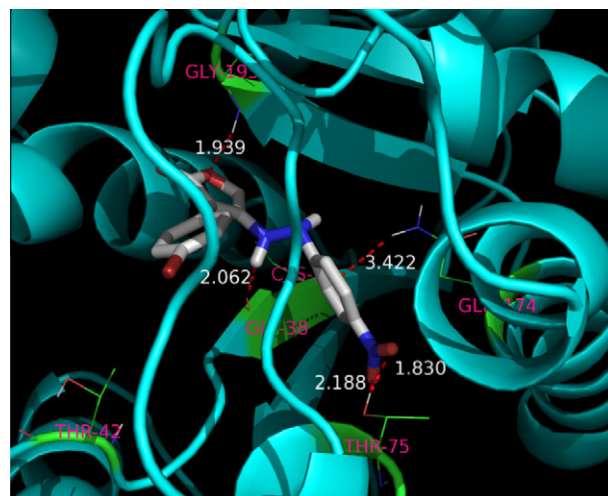


Figure 3. Binding mode of compound **4a11** with tyrosyl-tRNA synthetase from *S. aureus*. For clarity, only interacting residues were labeled. Hydrogen-bonding interactions are shown in dash. This figure was made using PyMol.

site of tyrosyl-tRNA synthetase might well explain its excellent inhibitory activity. On the other hand, our modeling results also

revealed that the hydrophobic 4-bromophenyl group sat in a hydrophilic pocket which is constructed by His47, His50, Lys84, Arg88, Asp195, and Gln196. This indicates that introduction of hydrophilic groups at this moiety may improve the antibacterial potency. For a definite conclusion, some compounds bearing hydrophilic groups as well as hydrophobic, electron withdrawing or electron donating groups in benzene ring at 3-position of furanone would be synthesized for antibacterial evaluation.

3. Conclusions

Thirty-one 3-aryl-4-alkylaminofuran-2(5H)-one derivatives were prepared and tested for their antimicrobial activities. Some of them showed good activities against Gram-positive organisms, and all of them were inactive against Gram-negative bacterium (*E. coli* ATCC 35218). Compound **4a11** showed the most potent antibacterial activity with MIC₅₀ of 0.42 µg/mL against *S. aureus* ATCC 25923. A positive correlation between the IC₅₀ values in the enzyme assay and the MIC₅₀ values against whole cell indicates that the possible action mechanism of the synthetic compounds might be due to their inhibitory activities against tyrosyl-tRNA synthetase. Molecular docking study revealed that various interactions tightly anchored **4a11** to the active site, which could well explain its excellent enzyme inhibitory and antibacterial activity. According to this modeling, a more suitable optimization strategy might be to modify the benzene ring at 3-position of furanone with hydrophilic groups and this work is undergoing.

4. Experiments

4.1. Antimicrobial activity

The antibacterial activities of the synthesized compounds was tested against two Gram-positive bacterial strains (*B. subtilis* ATCC 6633, *S. aureus* ATCC 25923, kanamycin as positive control) and a Gram-negative bacterial strain (*E. coli* ATCC 35218, penicillin as positive control) using LB medium. The antifungal activities of the compounds was tested against *C. albicans* ATCC 10231 (Gram-positive, ketoconazole as positive control) using RPMI-1640 medium. The MIC₅₀s of the test compounds were determined by a colorimetric method using the dye MTT.²² A stock solution of the synthesized compound (1000 µg/mL) in DMSO was prepared and graded quantities of the test compounds were incorporated in specified quantity of sterilized liquid medium (50% (v/v) of DMSO in PBS). A specified quantity of the medium containing the test compound was poured into 96-well plates. Suspension of the microorganism was prepared to contain approximate 10⁵ cfu/mL and applied to 96-well plates with serially diluted compounds to be tested and incubated at 37 °C for 24 h. In the case of fungi, plates were incubated at 27 °C for 48 h. Fifty microliters of PBS containing 2 mg of MTT/mL was added to each well. Incubation was continued at room temperature for 4–5 h. The content of each well was removed, and 100 µL of 10% sodium dodecyl sulfate containing 5% isopropanol and 1 mol/L HCl was added to extract the dye. After 12 h of incubation at room temperature, the optical density (OD) was measured with a microplate reader at 550 nm. The observed MIC₅₀s were presented in Table 3.

4.2. Preparation of the tyrosyl-tRNA synthetase and enzyme assay

S. aureus tyrosyl-tRNA synthetase was over-expressed in *E. coli* and purified to near homogeneity (~98% as judged by SDS-PAGE) using standard purification procedures.¹⁷ Tyrosyl-tRNA synthetase activity was measured by aminoacylation using modifications to previously described methods.¹⁶ The assays were performed at

37 °C in a mixture containing (final concentrations) 100 mM Tris/Cl pH 7.9, 50 mM KCl, 16 mM MgCl₂, 5 mM ATP, 3 mM DTT, 4 mg/mL *E. coli* MRE600 tRNA (Roche) and 10 µM L-tyrosine (0.3 µM L-[ring-3,5-³H] tyrosine (PerkinElmer, specific activity: 1.48–2.22 TBq/mmol), 10 µM carrier). Tyrosyl-tRNA synthetase (0.2 nM) was preincubated with a range of inhibitor concentrations for 10 min at room temperature followed by the addition of pre-warmed mixture at 37 °C. After specific intervals, the reaction was terminated by adding aliquots of the reaction mix into ice-cold 7% trichloroacetic acid and harvesting onto 0.45 mm hydrophilic Durapore filters (Millipore Multiscreen 96-well plates) and counted by liquid scintillation. The rate of reaction in the experiments was linear with respect to protein and time with less than 50% total tRNA acylation. IC₅₀s correspond to the concentration at which half of the enzyme activity is inhibited by the compound. The results were presented in Table 4.

4.3. Protocol of docking study

The automated docking studies were carried out using AutoDock version 4.2. First, AutoGrid component of the program precalculates a three-dimensional grid of interaction energies based on the macromolecular target using the AMBER force field. A grid box of 46 × 58 × 48 Å size (x, y, z) with a spacing of 0.375 Å and grid maps were created representing the catalytic active target site region where the native ligand was embedded. Then automated docking studies were carried out to evaluate the binding free energy of the inhibitor within the macromolecules. The genetic algorithm with local search (GA-LS) was chosen to search for the best conformers. The parameters were set using the software ADT (AutoDockTools package, version 1.5.4) on PC which is associated with AutoDock 4.2. Default settings were used with an initial population of 50 randomly placed individuals, a maximum number of 7.5 × 10⁶ energy evaluations, and a maximum number of 2.7 × 10⁴ generations. A mutation rate of 0.02 and a crossover rate of 0.8 were chosen. Results differing by less than 0.5 Å in positional root-mean-square deviation (RMSD) were clustered together and the results of the most favorable free energy of binding were selected as the resultant complex structures.

4.4. Crystallographic studies

X-ray single-crystal diffraction data for compound **4a9** was collected on a Bruker SMART APEX CCD diffractometer at 296(2) K using MoK α radiation (λ = 0.71073 Å) by the ω scan mode. The program SAINT was used for integration of the diffraction profiles. The structure was solved by direct methods using the SHELXS program of the SHELXL package and refined by full-matrix least-squares methods with SHELXL.²³ All non-hydrogen atoms of compound **4a9** were refined with anisotropic thermal parameters. All hydrogen atoms were generated theoretically onto the parent atoms and refined isotropically with fixed thermal factors.

4.5. Chemistry

All chemicals (reagent grade) used were purchased from Aldrich (U.S.A.) and Sinopharm Chemical Reagent Co., Ltd (China). Separation of the compounds by column chromatography was carried out with Silica Gel 60 (200–300 mesh ASTM, E. Merck). The quantity of silica gel used was 30–70 times the weight charged on the column. Then, the eluates were monitored using TLC. Melting points (uncorrected) were determined on a XT4 MP apparatus (Taike Corp., Beijing, China). ESI mass spectra were obtained on a Mariner System 5304 mass spectrometer, and ¹H NMR spectra were recorded on a Bruker DPX400 or DPX300 spectrometer at 25 °C with TMS and solvent signals allotted as internal standards. Chemical

shifts were reported in ppm (δ). Elemental analyses were performed on a CHN-O-Rapid instrument and were within $\pm 0.4\%$ of the theoretical values.

4.5.1. General procedure for preparation of compounds 1a–1f

An appropriately substituted phenylacetic acid (50 mmol) was added to a solution of sodium ethoxide (60 mmol) in ethanol (70 mL) and the mixture was stirred at 25 °C for 10 min. Ethyl bromoacetate (55 mmol) was added and the stirred mixture was heated under reflux temperature for 4–6 h. The precipitated salt was filtered off and the filtrate concentrated under reduced pressure. The resulted oil was dissolved in EtOAc and washed with water and brine. Then the solution was dried over MgSO_4 and concentrated under reduced pressure. The oily residue was then purified by column chromatography on silica gel to give **1a–1e** in yields of 75–88%.

4.5.2. General procedure for preparation of compounds 2a–2f

A dropwise solution of compound **1** (10 mmol) in dry THF (10 mL) was added to a suspension of NaH (24 mmol) in dry THF (20 mL) in an ice-cold bath and the stirring was maintained at room temperature for several hours (monitored by TLC). Water (30 mL) was added and the solution was extracted twice with ethyl ether. The aqueous phase was cooled to 0 °C and then acidified with concentrated hydrochloric acid to give a solid precipitate. Filtration and washing with water furnished compounds **2**. This material was used without further purification.

4.5.3. General procedure for preparation of compounds 3a–3f

Two milliliters of PCl_3 was added to 20 mL of DMF at 0 °C, after stirring for 10 min, followed by addition of 12 mL of dry ether. The mixture was stirred for further 10 min. Compound **2** (3 mmol) was then added and the mixture was stirred for 1–6 h at 5–10 °C. Thirty milliliters of saturated NaHCO_3 was dropwise added to quench the reaction and the solution was extracted thrice with EtOAc. Removal of solvent under reduced pressure gave a yellow solid which was used without further purification.

4.5.4. General procedure for preparation of 3-aryl-4-aminofuran-2(5H)-ones (**4**)

An appropriately substituted amine (0.6 mmol) was partially added to a solution of **3** (0.3 mmol) in dry THF (4 mL) at a temperature range of 0–10 °C. The reaction was quenched by addition of 10 mL water, and the solution was extracted thrice with EtOAc. After the solvent was removed under reduced pressure, the residue was purified by column chromatography on silica gel, eluting with EtOAc/petroleum ether (1:4–2:1, v/v).

4.5.4.1. 3-(4-Bromophenyl)-4-(pyrrolidin-1-yl)furan-2(5H)-one (4a1). Colorless crystal, 87%, mp 197–198 °C, ^1H NMR (CDCl_3): 1.81–1.99 (m, 4H); 3.15–3.26 (m, 4H); 4.74 (s, 2H); 7.16 (d, $J = 7.0$ Hz, 2H); 7.46 (d, $J = 7.2$ Hz, 2H); EIMS m/z 307 (M^+). Anal. Calcd for $\text{C}_{14}\text{H}_{14}\text{BrNO}_2$: C, 54.56; H, 4.58; Br, 25.93; N, 4.55. Found: C, 54.63; H, 4.57; Br, 25.87; N, 4.55.

4.5.4.2. 3-(4-Bromophenyl)-4-(piperidin-1-yl)furan-2(5H)-one (4a2). Colorless crystal, 93%, mp 145–147 °C, ^1H NMR (CDCl_3): 1.57–1.64 (m, 6H); 3.14 (t, $J = 5.2$ Hz, 4H); 4.75 (s, 2H); 7.17 (d, $J = 8.4$ Hz, 2H); 7.47 (d, $J = 8.1$ Hz, 2H); EIMS m/z 321 (M^+). Anal. Calcd for $\text{C}_{15}\text{H}_{16}\text{BrNO}_2$: C, 55.92; H, 5.01; Br, 24.80; N, 4.35. Found: C, 55.84; H, 5.01; Br, 24.86; N, 4.34.

4.5.4.3. 3-(4-Bromophenyl)-4-morpholinofuran-2(5H)-one (4a3).

Colorless crystal, 86%, mp 160–161 °C, ^1H NMR (CDCl_3): 3.18 (s, 4H); 3.67 (s, 4H); 4.77 (s, 2H); 7.17 (d, $J = 8.4$ Hz, 2H); 7.49 (d, $J = 8.0$ Hz, 2H); EIMS m/z 323 (M^+). Anal. Calcd for $\text{C}_{14}\text{H}_{14}\text{BrNO}_3$:

C, 51.87; H, 4.35; Br, 24.65; N, 4.32. Found: C, 51.95; H, 4.34; Br, 24.60; N, 4.31.

4.5.4.4. 3-(4-Bromophenyl)-4-(piperazin-1-yl)furan-2(5H)-one (4a4). Colorless crystal, 64%, mp 166–168 °C, ^1H NMR ($\text{DMSO}-d_6$): 2.66 (t, $J = 5.3$ Hz, 4H); 3.07 (t, $J = 5.0$ Hz, 4H); 4.90 (s, 2H); 7.81 (d, $J = 8.0$ Hz, 2H); 7.54 (d, $J = 8.0$ Hz, 2H); EIMS m/z 322 (M^+). Anal. Calcd for $\text{C}_{14}\text{H}_{15}\text{BrN}_2\text{O}_2$: C, 52.03; H, 4.68; Br, 24.72; N, 8.67. Found: C, 52.14; H, 4.69; Br, 24.66; N, 8.65.

4.5.4.5. 3-(4-Bromophenyl)-4-(2-morpholinoethylamino)furan-2(5H)-one (4a5). White powder, 71%, mp 132–134 °C, ^1H NMR (CDCl_3): 2.51 (t, $J = 4.6$ Hz, 4H); 2.63 (t, $J = 6.0$ Hz, 2H); 3.24 (dt, $J = 6.4$ Hz, $J = 5.3$ Hz, 2H); 3.74 (t, $J = 4.6$ Hz, 4H); 4.78 (s, 2H); 7.16 (d, $J = 8.2$ Hz, 2H); 7.47 (d, $J = 8.0$ Hz, 2H); EIMS m/z 366 (M^+). Anal. Calcd for $\text{C}_{16}\text{H}_{19}\text{BrN}_2\text{O}_3$: C, 52.33; H, 5.21; Br, 21.76; N, 7.63. Found: C, 52.38; H, 5.22; Br, 21.71; N, 7.62.

4.5.4.6. 3-(4-Bromophenyl)-4-(cyclohexylamino)furan-2(5H)-one (4a6). White powder, 75%, mp 166–167 °C, ^1H NMR (CDCl_3): 1.20–1.35 (m, 6H); 1.70–1.82 (m, 2H); 1.92–1.98 (m, 2H); 3.02–3.11 (m, 1H); 4.81 (s, 2H); 5.15 (br s, 1H); 7.34 (d, $J = 7.6$ Hz, 2H); 7.53 (d, $J = 6.9$ Hz, 2H); EIMS m/z 335 (M^+). Anal. Calcd for $\text{C}_{16}\text{H}_{18}\text{BrNO}_2$: C, 57.16; H, 5.40; Br, 23.77; N, 4.17. Found: C, 57.24; H, 5.41; Br, 23.74; N, 4.16.

4.5.4.7. 3-(4-Bromophenyl)-4-(propylamino)furan-2(5H)-one (4a7). Colorless crystal, 69%, mp 138–140 °C, ^1H NMR (CDCl_3): 0.98 (t, $J = 7.3$ Hz, 3H); 1.58–1.70 (m, 2H); 3.15 (q, $J = 6.8$ Hz, 2H); 4.78 (s, 2H); 5.32 (br s, 1H); 7.30 (d, $J = 7.8$ Hz, 2H); 7.49 (d, $J = 7.4$ Hz, 2H); EIMS m/z 295 (M^+). Anal. Calcd for $\text{C}_{13}\text{H}_{14}\text{BrNO}_2$: C, 52.72; H, 4.76; Br, 26.98; N, 4.73. Found: C, 52.79; H, 4.75; Br, 26.94; N, 4.72.

4.5.4.8. 3-(4-Bromophenyl)-4-(butylamino)furan-2(5H)-one (4a8). Colorless crystal, 63%, mp 98–100 °C, ^1H NMR (CDCl_3): 0.99 (t, $J = 7.3$ Hz, 3H); 1.33–1.47 (m, 2H); 1.56–1.67 (m, 2H); 3.15 (q, $J = 7.2$ Hz, 2H); 4.78 (s, 2H); 5.33 (br s, 1H); 7.27 (d, $J = 7.6$ Hz, 2H); 7.46 (d, $J = 7.2$ Hz, 2H); EIMS m/z 309 (M^+). Anal. Calcd for $\text{C}_{14}\text{H}_{16}\text{BrNO}_2$: C, 54.21; H, 5.20; Br, 25.76; N, 4.52. Found: C, 54.14; H, 5.21; Br, 25.73; N, 4.53.

4.5.4.9. 3-(4-Bromophenyl)-4-(dimethylamino)furan-2(5H)-one (4a9). Colorless crystal, 71%, mp 139–140 °C, ^1H NMR (CDCl_3): 3.27 (s, 6H); 4.78 (s, 2H); 7.28 (d, $J = 7.8$ Hz, 2H); 7.45 (d, $J = 7.4$ Hz, 2H); EIMS m/z 281 (M^+). Anal. Calcd for $\text{C}_{12}\text{H}_{12}\text{BrNO}_2$: C, 51.09; H, 4.29; Br, 28.32; N, 4.96. Found: C, 51.15; H, 4.28; Br, 28.35; N, 4.97.

4.5.4.10. 4-(Benzylamino)-3-(4-bromophenyl)furan-2(5H)-one (4a10). Colorless crystal, 89%, mp 220–221 °C, ^1H NMR ($\text{DMSO}-d_6$): 4.34 (d, $J = 6.4$ Hz, 2H); 4.81 (s, 2H); 7.24–7.39 (m, 5H); 7.43 (d, $J = 8.4$ Hz, 2H); 7.55 (d, $J = 8.6$ Hz, 2H); 8.16 (t, $J = 6.4$ Hz, 1H); EIMS m/z 343 (M^+). Anal. Calcd for $\text{C}_{17}\text{H}_{14}\text{BrNO}_2$: C, 59.32; H, 4.10; Br, 23.21; N, 4.07. Found: C, 59.25; H, 4.11; Br, 23.24; N, 4.06.

4.5.4.11. 3-(4-Bromophenyl)-4-(2-(4-nitrophenyl)hydrazinyl)furan-2(5H)-one (4a11). Yellow crystal, 59%, mp 220–223 °C, ^1H NMR ($\text{DMSO}-d_6$): 3.55 (s, 2H); 6.72 (d, $J = 9.1$ Hz, 2H); 7.29 (d, $J = 8.4$ Hz, 2H); 7.54 (d, $J = 8.4$ Hz, 2H); 8.04 (d, $J = 9.2$ Hz, 2H); 9.06 (s, 1H); 10.20 (s, 1H); EIMS m/z 389 (M^+). Anal. Calcd for $\text{C}_{16}\text{H}_{12}\text{BrN}_3\text{O}_4$: C, 49.25; H, 3.10; Br, 20.48; N, 10.77. Found: C, 49.18; H, 3.11; Br, 20.52; N, 10.75.

4.5.4.12. 4-(2-(4-Nitrophenyl)hydrazinyl)-3-phenylfuran-2(5H)-one (4b1). Red crystal, 63%, mp 203–205 °C, ^1H NMR (CDCl_3):

3.32 (s, 2H); 4.91 (s, 1H); 5.40 (d, $J = 8.9$ Hz, 2H); 5.53 (s, 1H); 5.80 (t, $J = 6.8$ Hz, 1H); 5.93 (t, $J = 7.5$ Hz, 2H); 6.00 (d, $J = 7.5$ Hz, 2H); 6.64 (d, $J = 9.0$ Hz, 2H); EIMS m/z 311 (M^+). Anal. Calcd for $C_{16}H_{13}N_3O_4$: C, 61.73; H, 4.21; N, 13.50. Found: C, 61.61; H, 4.21; N, 13.52.

4.5.4.13. 3-(4-Chlorophenyl)-4-(pyrrolidin-1-yl)furan-2(5H)-one (4c1). Colorless crystal, 77%, mp 182–184 °C, 1H NMR ($CDCl_3$): 1.81–1.98 (m, 4H); 3.13–3.24 (m, 4H); 4.74 (s, 2H); 7.20 (d, $J = 7.1$ Hz, 2H); 7.47 (d, $J = 7.4$ Hz, 2H); EIMS m/z 263 (M^+). Anal. Calcd for $C_{14}H_{14}ClNO_2$: C, 63.76; H, 5.35; Cl, 13.44; N, 5.31. Found: C, 63.85; H, 5.35; Cl, 13.42; N, 5.30.

4.5.4.14. 3-(3-Chlorophenyl)-4-(pyrrolidin-1-yl)furan-2(5H)-one (4d1). Colorless crystal, 96%, mp 128–130 °C, 1H NMR ($CDCl_3$): 1.85–1.97 (m, 4H); 3.11–3.30 (m, 4H); 4.74 (s, 2H); 7.17–7.28 (m, 4H); EIMS m/z 263 (M^+). Anal. Calcd for $C_{14}H_{14}ClNO_2$: C, 63.76; H, 5.35; Cl, 13.44; N, 5.31. Found: C, 63.87; H, 5.34; Cl, 13.42; N, 5.31.

4.5.4.15. 3-(3-Chlorophenyl)-4-(piperidin-1-yl)furan-2(5H)-one (4d2). White powder, 72%, mp 138–139 °C, 1H NMR ($CDCl_3$): 1.56–1.63 (m, 6H); 3.15 (t, $J = 5.7$ Hz, 4H); 4.75 (s, 2H); 7.18–7.23 (m, 1H); 7.24–7.27 (m, 2H); 7.28–7.32 (m, 1H); EIMS m/z 277 (M^+). Anal. Calcd for $C_{15}H_{16}ClNO_2$: C, 64.87; H, 5.81; Cl, 12.76; N, 5.04. Found: C, 64.79; H, 5.82; Cl, 12.74; N, 5.05.

4.5.4.16. 3-(3-Chlorophenyl)-4-morpholinofuran-2(5H)-one (4d3). Light yellow crystal, 97%, mp 177–178 °C, 1H NMR ($CDCl_3$): 3.19 (t, $J = 5.1$ Hz, 4H); 3.68 (t, $J = 4.8$ Hz, 4H); 4.78 (s, 2H); 7.17–7.21 (m, 1H); 7.27–7.31 (m, 3H); EIMS m/z 279 (M^+). Anal. Calcd for $C_{14}H_{14}ClNO_3$: C, 60.11; H, 5.04; Cl, 12.67; N, 5.01. Found: C, 60.24; H, 5.03; Cl, 12.64; N, 5.02.

4.5.4.17. 3-(3-Chlorophenyl)-4-(piperazin-1-yl)furan-2(5H)-one (4d4). White powder, 66%, mp 182–184 °C, 1H NMR ($DMSO-d_6$): 2.67 (t, $J = 5.2$ Hz, 4H); 3.09 (t, $J = 5.4$ Hz, 4H); 4.92 (s, 2H); 7.18–7.22 (m, 1H); 7.26–7.30 (m, 3H); EIMS m/z 278 (M^+). Anal. Calcd for $C_{14}H_{15}ClN_2O_2$: C, 60.33; H, 5.42; Cl, 12.72; N, 10.05. Found: C, 60.42; H, 5.43; Cl, 12.70; N, 10.03.

4.5.4.18. 3-(3-Chlorophenyl)-4-(4-methylpiperazin-1-yl)furan-2(5H)-one (4d5). Colorless crystal, 68%, mp 118–121 °C, 1H NMR ($CDCl_3$): 2.31 (s, 3H); 2.41 (t, $J = 5.1$ Hz, 4H); 3.22 (t, $J = 4.9$ Hz, 4H); 4.76 (s, 2H); 7.16–7.21 (m, 1H); 7.23–7.32 (m, 3H); EIMS m/z 292 (M^+). Anal. Calcd for $C_{15}H_{17}ClN_2O_2$: C, 61.54; H, 5.85; Cl, 12.11; N, 9.57. Found: C, 61.41; H, 5.86; Cl, 12.13; N, 9.58.

4.5.4.19. 3-(3-Chlorophenyl)-4-(2-morpholinoethylamino)furan-2(5H)-one (4d6). Light yellow crystal, 82%, mp 124–127 °C, 1H NMR ($CDCl_3$): 2.51 (t, $J = 4.6$ Hz, 4H); 2.63 (t, $J = 6.0$ Hz, 2H); 3.24 (dt, $J = 6.4$ Hz, $J = 5.3$ Hz, 2H); 3.74 (t, $J = 4.6$ Hz, 4H); 4.78 (s, 2H); 6.41 (br s, 1H); 7.19–7.25 (m, 1H); 7.36 (t, $J = 7.9$ Hz, 1H); 7.40–7.52 (m, 2H); EIMS m/z 322 (M^+). Anal. Calcd for $C_{16}H_{19}ClN_2O_3$: C, 59.54; H, 5.93; Cl, 10.98; N, 8.68. Found: C, 59.46; H, 5.94; Cl, 11.00; N, 8.69.

4.5.4.20. 3-(3-Chlorophenyl)-4-(propylamino)furan-2(5H)-one (4d7). Colorless crystal, 74%, mp 134–136 °C, 1H NMR ($CDCl_3$): 1.00 (t, $J = 7.3$ Hz, 3H); 1.59–1.71 (m, 2H); 3.14 (q, $J = 6.8$ Hz, 2H); 4.79 (s, 2H); 5.33 (br s, 1H); 7.20–7.24 (m, 1H); 7.30–7.36 (m, 2H); 7.44–7.47 (m, 1H); EIMS m/z 251 (M^+). Anal. Calcd for $C_{13}H_{14}ClNO_2$: C, 62.03; H, 5.61; Cl, 14.08; N, 5.56. Found: C, 61.96; H, 5.62; Cl, 14.10; N, 5.56.

4.5.4.21. 4-(Butylamino)-3-(3-chlorophenyl)furan-2(5H)-one (4d8). White powder, 74%, mp 90–94 °C, 1H NMR ($CDCl_3$): 0.97 (t, $J = 7.3$ Hz, 3H); 1.33–1.46 (m, 2H); 1.55–1.65 (m, 2H); 3.16 (q, $J = 7.2$ Hz, 2H); 4.79 (s, 2H); 5.32 (br s, 1H); 7.20–7.24 (m, 1H); 7.32–7.37 (m, 2H); 7.44–7.47 (m, 1H); EIMS m/z 265 (M^+). Anal. Calcd for $C_{14}H_{16}ClNO_2$: C, 63.28; H, 6.07; Cl, 13.34; N, 5.27. Found: C, 63.35; H, 6.06; Cl, 13.32; N, 5.28.

4.5.4.22. 4-(Benzylamino)-3-(3-chlorophenyl)furan-2(5H)-one (4d9). Colorless crystal, 89%, mp 120–122 °C, 1H NMR ($CDCl_3$): 4.39 (d, $J = 6.2$ Hz, 2H); 4.78 (s, 2H); 5.70 (br s, 1H); 7.20–7.24 (m, 1H); 7.26–7.30 (m, 2H); 7.31–7.44 (m, 5H); 9.48–7.51 (m, 1H); EIMS m/z 299 (M^+). Anal. Calcd for $C_{17}H_{14}ClNO_2$: C, 68.12; H, 4.71; Cl, 11.83; N, 4.67. Found: C, 68.23; H, 4.71; Cl, 11.81; N, 4.66.

4.5.4.23. 3-(3,4-Dimethoxyphenyl)-4-(pyrrolidin-1-yl)furan-2(5H)-one (4e1). Colorless crystal, 94%, mp 147–149 °C, 1H NMR ($CDCl_3$): 1.84–1.92 (m, 4H); 3.88 (s, 6H); 4.72 (s, 2H); 6.77–6.86 (m, 3H); EIMS m/z 289 (M^+). Anal. Calcd for $C_{16}H_{19}NO_4$: C, 66.42; H, 6.62; N, 4.84. Found: C, 66.34; H, 6.63; N, 4.84.

4.5.4.24. 3-(3,4-Dimethoxyphenyl)-4-(piperidin-1-yl)furan-2(5H)-one (4e2). Colorless crystal, 97%, mp 153–154 °C, 1H NMR ($DMSO-d_6$): 1.43–1.49 (m, 4H); 1.51–1.56 (m, 2H); 3.13 (t, $J = 5.0$ Hz, 4H); 3.73 (s, 3H); 3.75 (s, 3H); 4.85 (s, 2H); 6.74 (dd, $J = 8.5$ Hz, $J = 2.0$ Hz, 1H); 6.76 (d, $J = 2.0$ Hz, 1H); 6.92 (d, $J = 8.0$ Hz, 1H); EIMS m/z 303 (M^+). Anal. Calcd for $C_{17}H_{21}NO_4$: C, 67.31; H, 6.98; N, 4.62. Found: C, 67.23; H, 6.99; N, 4.62.

4.5.4.25. 3-(3,4-Dimethoxyphenyl)-4-morpholinofuran-2(5H)-one (4e3). Colorless crystal, 67%, mp 175–177 °C, 1H NMR ($DMSO-d_6$): 3.15 (t, $J = 5.0$ Hz, 4H); 3.57 (t, $J = 5.0$ Hz, 4H); 3.73 (s, 3H); 3.75 (s, 3H); 4.88 (s, 2H); 6.75 (dd, $J = 8.5$ Hz, $J = 2.0$ Hz, 1H); 6.77 (d, $J = 2.0$ Hz, 1H); 6.93 (d, $J = 8.0$ Hz, 1H); EIMS m/z 305 (M^+). Anal. Calcd for $C_{16}H_{19}NO_5$: C, 62.94; H, 6.27; N, 4.59. Found: C, 62.89; H, 6.27; N, 4.60.

4.5.4.26. 3-(3,4-Dimethoxyphenyl)-4-(piperazin-1-yl)furan-2(5H)-one (4e4). White powder, 61%, mp 122–124 °C, 1H NMR ($DMSO-d_6$): 2.66 (t, $J = 5.2$ Hz, 4H); 3.07 (t, $J = 5.4$ Hz, 4H); 3.72 (s, 3H); 3.75 (s, 3H); 4.93 (s, 2H); 6.74 (dd, $J = 8.4$ Hz, $J = 2.1$ Hz, 1H); 6.76 (d, $J = 2.0$ Hz, 1H); 6.94 (d, $J = 8.4$ Hz, 1H); EIMS m/z 304 (M^+). Anal. Calcd for $C_{16}H_{20}N_2O_4$: C, 63.14; H, 6.62; N, 9.20. Found: C, 63.22; H, 6.61; N, 9.18.

4.5.4.27. 4-(Cyclohexylamino)-3-(3,4-dimethoxyphenyl)furan-2(5H)-one (4e5). Colorless crystal, 73%, mp 124–125 °C, 1H NMR ($CDCl_3$): 1.15–1.41 (m, 6H); 1.73–1.84 (m, 2H); 1.91–1.99 (m, 2H); 3.01–3.12 (m, 1H); 3.89 (s, 3H); 3.90 (s, 3H); 4.81 (s, 2H); 5.17 (d, $J = 9.1$ Hz, 1H); 6.91 (s, 2H); 7.10 (s, 1H); EIMS m/z 317 (M^+). Anal. Calcd for $C_{18}H_{23}NO_4$: C, 68.12; H, 7.30; N, 4.41. Found: C, 68.20; H, 7.29; N, 4.42.

4.5.4.28. 3-(3,4-Dimethoxyphenyl)-4-(2-morpholinoethylamino)furan-2(5H)-one (4e6). White powder, 78%, mp 143–145 °C, 1H NMR ($CDCl_3$): 2.52 (t, $J = 4.6$ Hz, 4H); 2.66 (t, $J = 6.0$ Hz, 2H); 3.26 (dt, $J = 6.4$ Hz, $J = 5.3$ Hz, 2H); 3.75 (t, $J = 4.6$ Hz, 4H); 3.89 (s, 3H); 3.91 (s, 3H); 4.79 (s, 2H); 6.43 (br s, 1H); 6.76–6.84 (m, 3H); EIMS m/z 348 (M^+). Anal. Calcd for $C_{18}H_{24}N_2O_5$: C, 62.05; H, 6.94; N, 8.04. Found: C, 62.13; H, 6.93; N, 8.02.

4.5.4.29. 4-(Butylamino)-3-(3,4-dimethoxyphenyl)furan-2(5H)-one (4e7). White powder, 92%, mp 70–72 °C, 1H NMR ($CDCl_3$): 0.96 (t, $J = 7.3$ Hz, 3H); 1.32–1.45 (m, 2H); 1.52–1.63 (m, 2H); 3.14 (q, $J = 6.8$ Hz, 2H); 3.88 (s, 3H); 3.90 (s, 3H); 4.78 (s, 2H); 5.21 (br s, 1H); 6.90 (s, 2H); 7.10 (s, 1H); EIMS m/z 291 (M^+). Anal.

Calcd for $C_{16}H_{21}NO_4$: C, 65.96; H, 7.27; N, 4.81. Found: C, 65.85; H, 7.28; N, 4.81.

4.5.4.30. 4-(Benzylamino)-3-(3,4-dimethoxyphenyl)furan-2(5H)-one (4e8). Colorless crystal, 87%, mp 193–195 °C, 1H NMR ($CDCl_3$): 3.87 (s, 3H); 3.88 (s, 3H); 4.36 (d, J = 6.2 Hz, 2H); 4.78 (s, 2H); 5.60 (t, J = 6.0 Hz, 1H); 6.90 (d, J = 8.2 Hz, 1H); 6.94 (dd, J = 8.2 Hz, J = 1.8 Hz, 1H); 7.12 (d, J = 1.7 Hz, 1H); 7.25–7.44 (m, 5H); EIMS m/z 325 (M^+). Anal. Calcd for $C_{19}H_{19}NO_4$: C, 70.14; H, 5.89; N, 4.31. Found: C, 70.01; H, 5.90; N, 4.32.

4.5.4.31. 3-(3-Bromophenyl)-4-(dimethylamino)furan-2(5H)-one (4f1). White powder, 84%, mp 127–129 °C, 1H NMR ($CDCl_3$): 3.28 (s, 6H); 4.81 (s, 2H); 7.23 (t, J = 8.4 Hz, 1H); 7.33 (d, J = 8.4 Hz, 1H); 7.38 (d, J = 8.2 Hz, 1H); 7.43 (s, 1H); EIMS m/z 281 (M^+). Anal. Calcd for $C_{12}H_{12}BrNO_2$: C, 51.09; H, 4.29; Br, 28.32; N, 4.96. Found: C, 51.13; H, 4.29; Br, 28.33; N, 4.95.

Acknowledgments

The work was financed by Scientific Research Fund of Hunan Provincial Education Department (Project 09B083) of China, by a Grant (Project JSDXKYZZ0801) from Jishou University for talent introduction, China and by aid program for Science and Technology Innovative Research Team (Chemicals of Forestry Resources and Development of Forest Products) in Higher Educational Institutions of Hunan Province.

References and notes

- Masip, I.; Pérez-Payá, E.; Messegue, A. *Comb. Chem. High Throughput Screening* **2005**, *8*, 235.
- Barker, J. J. *Drug Discovery Today* **2006**, *11*, 391.
- Xiao, Z.-P.; Xue, J.-Y.; Tan, S.-H.; Li, H.-Q.; Zhu, H.-L. *Bioorg. Med. Chem.* **2007**, *15*, 4212.
- Xiao, Z.-P.; Fang, R.-Q.; Li, H.-Q.; Xue, J.-Y.; Zheng, Y.; Zhu, H.-L. *Eur. J. Med. Chem.* **2008**, *43*, 1828.
- Cotelle, P.; Cotelle, N.; Teissier, E.; Vezin, H. *Bioorg. Med. Chem.* **2003**, *11*, 1087.
- Lattmann, E.; Dunn, S.; Niamsanit, S.; Sattayasai, N. *Bioorg. Med. Chem. Lett.* **2005**, *15*, 919.
- Weber, V.; Rubat, C.; Duroux, E.; Lartigue, C.; Madesclaire, M.; Coudert, P. *Bioorg. Med. Chem.* **2005**, *13*, 4552.
- Weber, V.; Coudert, P.; Rubat, C.; Duroux, E.; Vallee-Goyet, D.; Gardette, D.; Bria, M.; Albuissou, E.; Leal, F.; Gramain, J. C.; Couquelet, J.; Madesclaire, M. *Bioorg. Med. Chem.* **2002**, *10*, 1647.
- Campbell, A. C.; Maidment, M. S.; Pick, J. H.; Stevenson, D. F. M. *J. Chem. Soc., Perkin Trans. 1* **1985**, 1567.
- Verniest, G.; De Kimpe, N. *Synlett* **2005**, 0947.
- Harrison, W. T. A.; Kumar, C. S. C.; Yathirajan, H. S.; Ashalathac, B. V.; Narayana, B. *Acta Crystallogr., Sect. E* **2010**, *66*, o2477.
- Ali, M. A.; Ismail, R.; Tan, S. C.; Yeap, C. S.; Fun, H.-K. *Acta Crystallogr., Sect. E* **2010**, *66*, o2531.
- Guzel, I. A.; Langenhan, J. M.; Chung, Y. J. *Acta Crystallogr., Sect. E* **2002**, *58*, o65.
- Burkhardt, A.; Eriksson, L.; Widmalm, G.; Cumpstey, I. *Acta Crystallogr., Sect. E* **2009**, *65*, o633.
- Qiu, X.; Janson, C. A.; Smith, W. W.; Green, S. M.; McDevitt, P.; Johanson, K.; Carter, P.; Hibbs, M.; Lewis, C.; Chalker, A.; Fosberry, A.; Lalonde, J.; Berge, J.; Brown, P.; Houge-Frydrych, C. S.; Jarvest, R. L. *Protein Sci.* **2001**, *10*, 2008.
- Berge, J. M.; Broom, N. J. P.; Houge-Frydrych, C. S. V.; Jarvest, R. L.; Mensah, L.; McNair, D. J.; O'hlanlon, P. J.; Pope, A. J.; Rittenhouse, S. J. *Antibiot.* **2000**, *53*, 1282.
- Stefanska, A. L.; Coates, N. J.; Mensah, L. M.; Pope, A. J.; Ready, S. J.; Warr, S. R. J. *Antibiot.* **2000**, *53*, 345.
- Ibba, M.; Söll, D. *Annu. Rev. Biochem.* **2000**, *69*, 617.
- Farhanullah; Kang, T.; Yoon, E.-J.; Choi, E.-C.; Kim, S.; Lee, J. *Eur. J. Med. Chem.* **2009**, *44*, 239.
- Jarvest, R. L.; Berge, J. M.; Berry, V.; Boyd, H. F.; Brown, M. J.; Elder, J. S.; Forrest, A. K.; Fosberry, A. P.; Gentry, D. R.; Hibbs, M. J.; Jaworski, D. D.; O'Hanlon, P. J.; Pope, A. J.; Rittenhouse, S.; Sheppard, R. J.; Slater-Radosti, C.; Worby, A. J. *Med. Chem.* **2002**, *45*, 1959.
- Hudson, I. R. J. *Hosp. Infect.* **1994**, *27*, 81.
- Chiou, C. C.; Mavrogiorgos, N.; Tillem, E.; Hector, R.; Walsh, T. J. *Antimicrob. Agents Chemother.* **2001**, *45*, 3310.
- Sheldrick, G. M. *SHELXTL-97*; University of Göttingen: Göttingen, Germany, 1997.